OPTOELECTRONICS AND ADVANCED MATERIALS – RAPID COMMUNICATIONS Vol. 1, No. 4, April 2007, p. 158 - 161

# Strength control in multiple optical traps generated by means of diffractive optical elements

ALI-REZA MORADI[a], E. FERRARI[b,c], V. GARBIN[b,c], E. DI FABRIZIO[b,d], D. COJOC[b,e*]
[a]*Institute for Advanced Studies in Basic Sciences, Gava Zang, Zanjan 45195-1159, Iran*
[b]*CNR - Istituto Nazionale per la Fisica della Materia, Laboratorio Nazionale TASC Area Science Park – Basovizza, S.S. 14 Km 163.5, 34012 Basovizza (TS), Italy*
[c]*University of Trieste, Department of Physics, Via Valerio 2, 34027 Trieste, Italy*
[d]*University of Magna Graecia, Viale Europa, Campus Germaneto (CZ), Italy*
[e]*University Politehnica of Bucharest, Optoelectronics Research Center, 1-3 Bd Iuliu Maniu, Bucharest, Romania*

We present a simple technique to generate arrays of optical traps with different trapping forces. The arrays can be configured in two or three dimensions (2D, 3D) by means of phase diffractive optical elements (DOEs) displayed on a phase programmable modulator. DOEs design is based on the approach of spherical wave propagation and superposition, which enables to individually control the strength of the optical trap. Experimental results using silica beads trapped with different forces in 2D and 3D configurations are presented.

(Received February 27, 2007; accepted March 14, 2007)

*Keywords:* Optical confinement and manipulation, Binary optics, Laser beam shaping, Microscopy, Spatial light modulators

## 1. Introduction

One of the most exciting developments in optical tweezers in recent years has been the creation of 2D and 3D arrays of traps for multiple particle trapping and independent manipulation of the trapped particles. Three main techniques have been introduced originally to this purpose: fast scanning of the laser beam [1], phase to intensity pattern conversion by generalized phase contrast (GPC) method using spatial light modulators (SLMs) [2] and laser beam shaping by means of diffractive optical elements (DOEs) displayed on SLMs [3,4,5].

Scanned optical tweezers can trap multiple particles in 2D arrays by dwelling briefly on each trap before moving onto the next. Such a system, which enables also an independent control of the trapping force for each trap of the pattern by adjusting the dwelling time, has been recently demonstrated [6].

3D trapping and manipulation of polystyrene micro beads, based on the GPC method in a counter-propagating beams system, has been proposed recently [7]. Objectives with low NA are used in this system and, therefore, a wider manipulation region, a larger depth of field and an additional orthogonal direction for imaging can be obtained. Nevertheless, attention should be paid using low NA objectives since manipulation can not be achieved with high resolution, which might be a must for certain applications. Moreover, the two objective configuration is incompatible with some microscopy techniques, e.g. differential interference contrast (DIC), and limits the possibility to mount on the upper part of the microscope additional tools as micromanipulators or microinjectors required in biological applications.

The use of DOEs allows to obtain multiple trapping and manipulation in 2D and 3D arrays with only one beam. Many improvements and applications of this technique have been proposed after the first demonstrations of the working principle. The use of iterative techniques based on Gerchberg-Saxton algorithm [8] has been extended from 2D pattern to 3D beam shaping [9,10] and allowed to create large number of high-quality optical traps with different configurations and different modes of light [11]. Recently, another iterative technique based on direct binary search, has been demonstrated for optimizing traps efficiency and accuracy [12] and applied to the study of thermally driven vibrations in a one-dimensional hydrodynamically coupled colloidal crystal [13]. The above mentioned techniques guarantee very good control over the trap but might require a high number of iterations until the optimum solution is reached.

A simple non-iterative method, based on the propagation and superposition of spherical waves, has been used by us to design DOEs for 3D multi trapping [14] and demonstrate simultaneously three dimensional optical sectioning and optical manipulation of living cells [15]. The system combines multi trap OT with a video microscope to enable axial scanning of living cells while maintaining the trapping configuration at a fixed position. This is achieved compensating the axial movement of the objective by shaping the wave front of the trapping beam with proper DOEs displayed on SLM.

In this paper we address the strength control of the optical traps configured in 2D and 3D arrays by means of phase DOEs. We propose a modification of the algorithm based on the spherical wave approach, which enables to calculate phase DOEs that generate optical traps with different strength. The strength control is demonstrated experimentally with 1.5 μm diameter silica beads.

## 2. DOE's design based on the spherical wave approach

Phase DOEs are known as optical elements that convert the input (illuminating) wave, by modulating only its phase, into a wave with desired distribution of amplitude, phase or polarization. Among the various techniques to calculate the function of a phase DOE, here we propose a modified version of the original algorithm based on spherical wave propagation and superposition approach [14].

In the spherical wave approach we assume that both the light source, which illuminates the DOE, and the generated pattern can be described by point sources that emit spherical waves. The phase function of the DOE is obtained from the propagation and superposition of the spherical wavefronts reaching the plane of the DOE. If we consider the DOE as a thin phase element described by its function $t(x,y)=\exp[i\varphi(x,y)]$ and the complex amplitude $W_{in}(x,y;z=0)=a_{in}(x,y)\exp[i\varphi_{in}(x,y)]$ of the input wave, the complex amplitude $W_{out}(x,y;z=0)=a_{out}(x,y)\exp[i\varphi_{out}(x,y)]$ of the output wave right away the DOE will be:

$$W_{out}(x,y;z=0)=t(x,y)W_{in}(x,y;z=0) \qquad (1)$$

where z=0 denotes the DOE plane. If $\{P_s\ (x_s,y_s;z_s),\ s=1..N_s\}$ is the set of $N_s$ points describing the light source and $\{P_g\ (x_g,y_g;z_g),\ g=1..N_g\}$ is the set of $N_g$ points describing the generated spots, the complex amplitudes of the input and output waves at a given point P(x,y;z=0) of the DOE can be calculated considering spherical wave propagation and superposition:

$$W_{in(out)}(x,y;z=0)=\sum_{s=1(g=1)}^{N_s(N_g)} a_{s(g)}\cos\psi_{s(g)}\exp\left(ikr_{s(g)}\right)/r_{s(g)} \qquad (2)$$

where $a_{s(g)}$ are the amplitudes of the spherical waves emitted by the point sources, $\cos\psi_{s(g),d}=z_{s(g)}/r_{s(g)}$ is the obliquity factor, $r_{s(g),d}$ is the distance between the point source $P_{s(g)}$ and the given point $P_d$ of the DOE and k is the wave number, $k=2\pi/\lambda$. Knowing the complex amplitudes of the input and output wavefronts, an estimate of the DOE's phase function, $\varphi(x,y)$ can be obtained by subtracting the phase of the input wave from the phase of the output wave. The result is correct when the modulus of the input and output waves are identical in all the points of the DOE. Although this condition can not be reached in general, the result represents already a good estimate of the phase function. In our previous applications [14,15], all the spherical waves emitted by the point sources were considered to have the same amplitude. This assumption was sufficient to get the required optical function of the DOE for the respective applications.

Assigning different amplitudes $a_g$, to the spherical waves in Eq. (2) one can control the intensity of the spots generated by the DOE and hence the strength of the corresponding optical traps. To illustrate better this idea, let us consider the following example: a DOE which, illuminated by a plane, wave generates a 3×3 array of spots, as shown in Fig. 1a. All the spots have to be generated in a plane z= 500 mm after the DOE. The intensity of the spots in the second and third columns is respectively two and three times higher than the intensity of the spots in the first column, as shown in Fig. 1d (black line) and the spacing between the spots is d= 1 mm. Since the DOE is illuminated by a plane wave ($N_s$=1, $r_s$ --> infinity), the complex amplitude distribution $W_{in}$ in Eq. (2) will be constant over the DOE. On the other side, the complex amplitude distribution $W_{out}$ is calculated with the weighting coefficients: $a_g$=1 (for g=1,2,3), $a_g$=2 (for g=4,5,6), $a_g$=3 (for g=7,8,9). Because of the plane wave illumination, the phase $\varphi_{out}$ of the complex amplitude distribution, $W_{out}$ already represents the phase function of the DOE ($\varphi=\varphi_{out}$). A 256×256 pixels detail of the central part of the DOE is shown in Fig. 1b (eight grey scales represent eight phase levels in the range 0–2π).

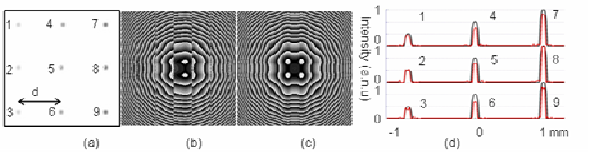


*Fig. 1. (a) The desired 3×3 array of spots with three different intensities; (b) detail of the calculated phase DOE (eight phase levels); (c) detail of the phase DOE calculated to generated the same array but with the same intensity in each spot; (d) intensity profiles (computer simulated) along the three lines containing the spots: black – desired, red – obtained with the DOE in (b).*

For comparison, the phase function of the DOE which generates the same array but with uniform intensity for all the spots is shown in Fig. 1c. Profiles of the intensity distribution calculated at z= 500 mm after the DOE in Fig 1b, are depicted (red line) in Fig. 1d together with the desired intensity profiles. One can see that the calculated profiles fit almost perfectly the desired profiles. The small differences might be due to the errors introduced by mismatching the amplitude of the input wave (constant over the DOE) and the amplitude of the output wave. This does not affect the validity of the designing approach and can be corrected if necessary by adjusting the weighting coefficients $a_g$ after the first experimental results are analyzed. Using a higher number of weighting coefficients will allow finely tunning for different intensity levels in the spots. This approach allows also to calculate DOEs that generate arrays of spots arranged in 3D configurations, by changing the coordinates $z_g$ correspondingly in Eq 2.

## 3. Experimental results

We have tested the DOE design technique described in section 2 by implementing the DOEs on a phase programmable modulator (PPM) in an optical trapping setup. The setup is based on a standard inverted microscope (Nikon TE2000-E) with a 100×, 1.4 NA oil immersion objective. The path of the laser beam is represented in Fig. 2.

We use a single mode CW fiber laser (L) (IPG Fibertech PYL-M-10-LP) that generates a collimated linear polarized beam at 1064 nm. This is then expanded by a 3× expander (E) to match the active area of the phase programmable modulator (PPM) (Hamamatsu PPM-X8267). This is an electrically-addressed SLM using an

optical image transmitting element to couple an optically-addressed PAL-SLM (Parallel Aligned nematic Liquid crystal SLM) with an electrically addressed intensity modulator and allows to control the phase of the input beam over an area of 2×2 $cm^2$ (768×768 pixels) providing a 2π phase shift at 1064 nm. The calculated phase DOE displayed on the PPM splits and focuses the beam into the focal plane F. The beam is then reflected by the dichroic mirror (DM) to the microscope objective (MO) and focused by it into the working plane (WP) placed at distance $z_p$ from the focal plane (FO) of the MO.

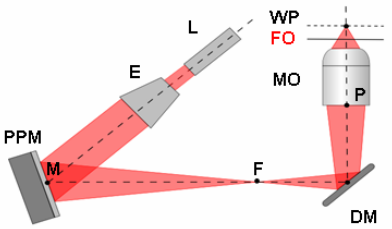


*Fig. 2. The light path of the laser beam: L – fiber laser; E – 3× beam expander; PPM – programmable phase modulator; DM – dichroic mirror; MO – microscope objective; FO – microscope objective's focal plane; WP – working plane.*

The planes F and WP are conjugated planes, therefore the distance $z_p$ can be defined by the Newton equation:

$$z_P = f_0^2/z \qquad (3)$$

where $f_o$ is the focal length of the MO and z= FP is the distance from plane F to the first focal plane of the MO which is located approximately in the entrance pupil of the MO. Since the position of the plane F is defined by the DOE, the position $z_p$ of the working plane can be easily controlled in the range 0-20 μm by changing the focal length (f= MF) of the DOE displayed on the PPM. The beam can be also focused at different distances f by the same DOE, thus allowing to generate 3D array of traps near the focal plane FO of the MO. The calibration ($z_p$-f-z) that allows to control the position of the traps is described in detail in Reference [15]. Since the WP might be far from the FO, the image may be moved from the standard imaging plane (one of the exit ports) inside the microscope, where the image detector (we use a CMOS camera EPIX silicon video 1281) cannot be inserted. Therefore we built a telescope-like system to transport the image outside the microscope for imaging. This imaging solution (not shown in Fig. 2) is similar to that reported in Ref 15.

For our trapping experiments we have used a sample cell built with two microscope slides and filled with 1.5 μm diameter silica beads immersed in water ($10^{-2}$% w/v). Phase DOEs (768×768 pixels, 8 phase levels) were calculated to fill the active area of the PPM. We test our DOE design approach to generate multi force optical traps in two different experiments: in the first we consider a 2D array with three different trapping forces as the example discussed in section 2; in the second we consider a 3D array with two different trapping forces.

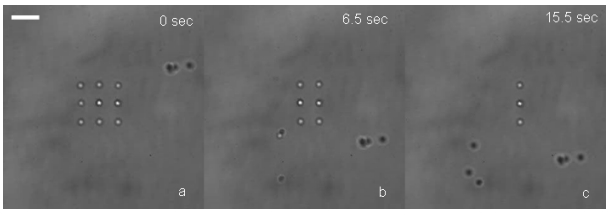


*Fig. 3. a) 2D array of 3×3 microbeads trapped with different trapping forces: moving the microscope stage with a low velocity all the beads remain trapped; increasing the velocity (see Fig. 4) the beads of the first (b) and second (c) column are removed from the traps, showing different trapping forces.*

A 2D array (15 μm×15 μm) of 3×3 trapped micro beads is shown in Fig. 3a. The power at the output of the laser was P= 800 mW and considering the losses of the optical system we estimate the power of the beam in the focal plane of the microscope objective $P_f$ = 80 mW. From the point of view of the trapping strength, the first column should be the weakest, the second and the third columns being respectively two and three times stronger. This is tested by moving the sample cell fixed on the microscope stage with variable velocity and by video tracking the beads escaping from the traps (Fig. 3).

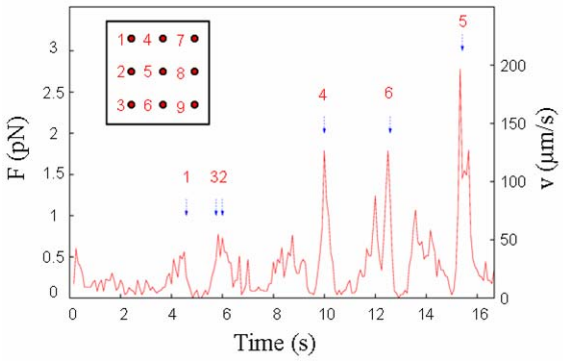


*Fig. 4. Relative velocity bead-water, drag force and trapping force for the array of 3×3 traps. Beads 1, 2 and 3 escape from the traps for forces approximately two times lower than beads 4 and 6. Bead 5 escapes for a higher force since its trap is strengthen by the zero order. The inset shows the numbering for the nine beads trapped.*

The lateral trapping force is estimated to be the minimum external force required to dislodge the particle from the trap. By moving the microscope stage, the Stokes drag force exerted by the fluid on the trapped particle is:

$$F_{Stokes} = 3\pi\eta dv \qquad (4)$$

where η is the viscosity of the fluid (η= $10^{-3}$ $Ns/m^2$ for water), d= 1.5 μm is the diameter of the trapped particle and v is the relative velocity bead-fluid imposed by the movement of the microscope stage. This movement is recorded (12 fps) and by tracking a fixed particle on the coverslip we calculate the relative velocity bead-water. When the velocity v exceeds a certain value, the drag force

becomes bigger than the trapping force and the bead is moved away from the optical trap. The velocity and the drag force for the 3×3 array of trapped micro beads during the experiment shown in Fig. 3 are represented in Fig. 4. The measured velocities and forces corresponding to the moment in which the beads escape from the first two column of traps are: first column ($v_1$= 39.5 μm/s, $F_1$= 0.56 pN; $v_2$= 51.4 μm/s, $F_2$= 0.73 pN; $v_3$= 54.7 μm/s, $F_3$= 0.77 pN), second column ($v_4$= 126.6 μm/s, $F_4$= 1.79 pN; $v_5$= 196.9 μm/s, $F_5$= 2.78 pN; $v_6$= 126.3 μm/s, $F_6$= 1.79 pN). These values show that the trapping strength is increased from the first column to the third column. Nevertheless, the trapping forces are not proportional, as shown by the simulations: the trapping forces for the second column are more than two times stronger than those corresponding to the first column and the trapping force of the central bead (5) is 1.56 times stronger than those corresponding to the other two beads in the second column. This difference is due to the effective intensity of the spots, which is very sensitive to the alignment and the size of the apertures in the optical path. By measuring the intensity distribution over the 3×3 spots before trapping we observed the concordance with the velocity and force measurements after trapping. The central trap (5) is strengthen by additional light corresponding to the focused zero order. This problem can be avoided by modifying the optical train of the setup (e.g. changing the convergence of the input beam [11]). Alternatively, a better calibration of the forces can be obtained by adjusting the weighting coefficients $a_g$ and the distances $z_g$ in Eq 2.

The same approach allows generating also 3D arrays of traps with different trapping forces. An array of 4 traps arranged on two different planes (separated by 6 μm) with two different trapping forces in each plane is shown in Fig. 5. The beads are first trapped and than the microscope stage is moved to prove the trapping forces. The beads from the weakest traps (one in each plane) escape almost simultaneously at v= 64 μm/s (F= 0.9 pN).

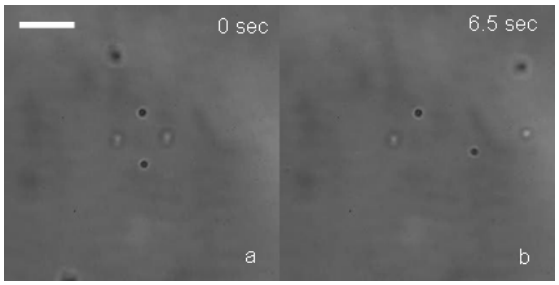


*Fig. 5. a) 3D array of 2×2 microbeads arranged in two different planes and trapped with two different trapping forces. b) The beads from the weakest traps escape when the microscope stage is moved fast enough (v=64 μm/s, F=0.9 pN); scale bar 10 μm.*

## 4. Conclusions

In conclusion, we demonstrate that gradient of forces can be obtained for 2D and 3D arrays of traps by means of phase DOEs calculated with a non-iterative algorithm based on a modified version of the spherical wave approach. Different trapping strength is obtained by weighting the coefficients which describe the intensity of the point sources generating spherical waves. Three levels for the trapping force are demonstrated. A higher number of levels can be introduced to finely tune the forces in an adaptive trapping experiment.

**Acknowledgements**

The authors thank Dr. Miltcho Danailov from the Laser Lab of the Elettra Synchrotron, Trieste, for valuable discussion. AR Moradi acknowledges the support of Abdus Salam ICTP (International Center for Theoretical Physics), Trieste, Italy – the Sandwich Training Educational Program (STEP).

## References

[1] K. Sasaki, M. Kashioka, H. Misawa, N. Kitamura, H. Masuhara, Opt. Lett. **16**, 1463-1465 (1991).
[2] R. L. Eriksen, P. C. Mogensen, J. Glückstad, Opt. Lett. **27**, 267-269 (2002).
[3] E. R. Dufresne, D. G. Grier, Rev. Sci. Instr. **69**, 1974–1977 (1998).
[4] J. Liesener, M. Reicherter, T. Haist, H. J. Tiziani, Opt. Commun. **185**, 77-82 (2000).
[5] E. Dufresne, G. C. Spalding, M. T. Dearing, S. A. Sheets, D. G. Grier, Rev. Sci. Instrum. **72**, 1810-1816 (2001).
[6] V. Emiliani, D. Sanvitto, M. Zahid, F. Gerbal, M. Coppey-Moisan, Opt. Express **12**, 3906-3910 (2004), http://www.opticsexpress.org/abstract.cfm?URI=OPEX-12-17-3906.
[7] I. R. Perch-Nielsen, P. J. Rodrigo, J. Glückstad, Opt. Express **13**, 2852-2857 (2005), http://www.opticsexpress.org/abstract.cfm?URI=OPEX-13-8-2852 .
[8] R. W. Gerchberg, W. O. Saxton, Optik **35**, 237-246 (1972).
[9] G. Sinclair, P. Jordan, J. Courtial, M. Padgett, J. Cooper, Z. J. Laczik, Opt. Express **12,** 5475-5480 (2004). http://www.opticsexpress.org/abstract.cfm?URI=OPEX-12-22-5475.
[10] G. Whyte, J. Courtial, New J. Phys. **7**, 117 (2005) http://ej.iop.org/links/q76/YTTBDwYbHw767CUP0VhqAg/njp5_1_117.pdf .
[11] J. E. Curtis, B. A. Koss, D. G. Grier, Opt. Commun. **207**, 169-175 (2002).
[12] Marco Polin, Kosta Ladavac, Sang-Hyuk Lee, Yael Roichman, David G. Grier, Opt. Express **13,** 583-5845 (2005).
[13] Marco Polin, David G. Grier, Stephen R. Quake, PRL 96, 088101 (2006).
[14] D. Cojoc, V. Emiliani, E. Ferrari, R. Malureanu, S. Cabrini, R. Zacharia, E. Di Fabrizio, Jpn. J. Appl. Phys. **43**, 3910-3915 (2004).
[15] V. Emiliani, D. Cojoc, E. Ferrari, V. Garbin, C. Durieux, M. Coppey-Moisan, E. Di Fabrizio, Opt. Express **13,** 1395-1405 (2005).

*Corresponding author: cojoc@tasc.infm.it